



PERFORMANCE OF NANOPOROUS FILTRATION MEMBRANE WITH CONICAL PORES: FOR A LIQUID-PARTICLE SEPARATION

Yongbin Zhang*

College of Mechanical Engineering, Changzhou University, Changzhou, 213164, Jiangsu Province, China

ABSTRACT

An analysis was developed for the flow resistance of the nanoporous filtration membrane with conical pores for a liquid-particle separation, based on the nanoscale flow model. The calculation results show that there exists the optimum cone angle of the conical pore which gives the lowest flow resistance and thus the highest flux of the membrane; This optimum cone angle of the conical pore depends on the radius of the small opening of the conical pore, the passing liquid-pore wall interaction and the membrane thickness. The equations were regressed out for calculating this optimum cone angle respectively for weak, medium and strong liquid-pore wall interactions. For the optimum cone angle of the conical pore, the dimensionless minimum flow resistance of the membrane was calculated and it is only dependent on the radius of the small opening of the conical pore and the passing liquid-pore wall interaction.

Keywords: Membrane; Filtration; Nanopore; Flow; Mode

1. INTRODUCTION

Nanoporous filtration membranes have been successfully applied in super purification, hemofiltration, drug delivery, DNA analysis, biosensing and biotechnology (Adiga et al., 2009; Biffinger et al., 2007; Desai et al., 2000; Escosura-Muniz and Merkoç, 2011; Fissel et al., 2009; Hinds et al., 2004; Jackson and Hillmyer, 2010). They are in fast progress especially in manufacturing. Currently, the pores taken in such membranes can be single cylindrical, double cylindrical or single conical (Baker and Bird, 2008; Vlassioug et al., 2009; Zhang, 2018a). It was found that both double cylindrical pores and single conical pores are advantageous over single cylindrical pores owing to yielding the higher fluxes of the membranes (Vlassioug et al., 2009; Zhang, 2018a).

Nanoporous filtration membranes with conical pores have been studied plentifully by experiments. Scopece *et al.* (2006) found that the cone angle of the pore in this membrane can be well controlled by controlling the amount of the ethanol present in an alkaline etching solution. Vlassioug *et al.* (2009) showed that the radius of the conical pore is linearly increased with the increase of the etching time; they also showed that both the porosity of the membrane and the pore surface chemistry can be well controlled when manufacturing the SiN membranes by the ion track-etching technique. Harrell *et al.* (2006) found that the cone angle of the pore can be changed by varying the trans-membrane potential difference in pore etching. Mukaibo *et al.* (2009) found that the length of the conical pore was linearly increased with the increase of the etch time when the etch temperature was low.

Theoretical analysis for the performance of nanoporous filtration membranes was less seen in the past. Cervera *et al.* (2005) developed an analysis for the ionic transport through synthetic conical nanopores based on the Poisson and Nernst-Planck equations. Zhang (2018a-c) analytically studied the performances of nanoporous filtration membranes respectively with double cylindrical pores and tree-type cylindrical pores based on the flow equation for a nanoscale flow. He

found the optimum working conditions of these membranes in which the fluxes of the membranes are the highest. He also developed the design principles for these membranes.

The present paper aims to develop an analysis for the performance of a nanoporous filtration membrane with conical pores which is for a liquid-particle separation, based on the flow equation for a nanoscale flow. This is the pioneering theoretical study on such membranes with non-electrokinetic flows, although the experimental studies on them have been plentiful. The flow resistance of the membrane was calculated in this study for different geometrical shapes of the pore and different passing liquid-pore wall interactions. The optimum cone angle of the pore was found for the lowest flow resistance i.e. the highest flux of the membrane. The equations for calculating this optimum cone angle of the pore were regressed out respectively for weak, medium and strong liquid-pore wall interactions. The equations for the corresponding lowest flow resistances of the membrane were also derived. The present study should be of significant interest to the understanding of the performance of a nanoporous filtration membrane with conical pores for a liquid-particle separation and to the design of this membrane.

2. STUDIED MEMBRANE

Figures 1(a) and (b) show the studied nanoporous filtration membrane with conical pores. The pore is identical and uniformly distributed within the membrane. The radii of the small and large openings of the pore are respectively R_0 and R_1 , the cone angle of the pore is θ , and the thickness of the membrane is l . The property of the pore wall surface is uniform. The membrane is for a liquid-particle separation. The value of R_0 is determined according to the requirement of the particle filtration. The membrane thickness l is determined according to the requirement of the mechanical strength of the membrane. The cone angle θ can be optimized for giving the highest flux of the membrane.

*Email: engmech1@sina.com

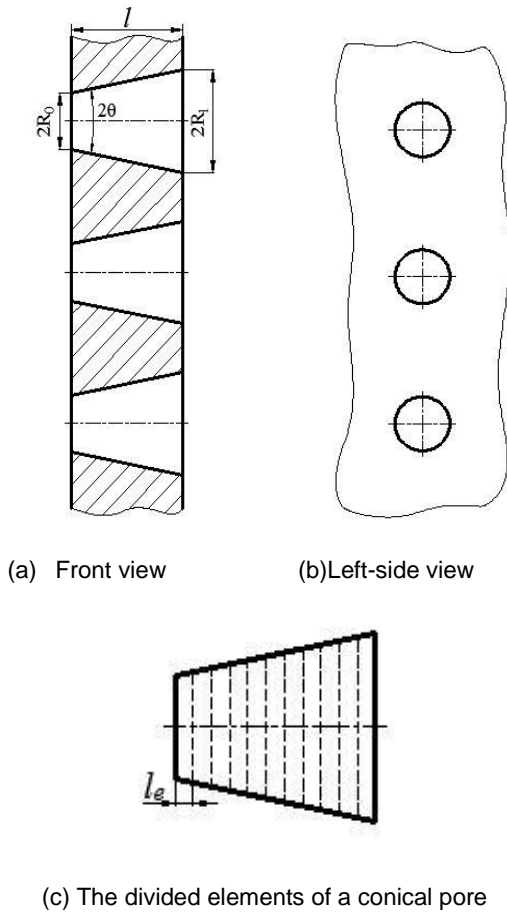


Fig. 1 The studied nanoporous filtration membrane with conical pores.

3. ANALYSIS

The analysis for the flow in the nanopore of the membrane is based on the flow equation for a nanoscale flow (Zhang, 2016). For the analysis feasibly carried out, a conical pore is divided into n elementary very small sections with the same axial length l_e , as shown in Fig.1(c). When n is sufficiently large, a divided elementary section of the pore can be taken as a cylindrical pore with the axial length l_e ; While, the radius of this equivalent cylindrical pore is equal to the mean radius of the divided elementary section of the conical pore. It is easily written that $l_e = l/n$ and $R_{1,i} = R_0 + i l_e \tan\theta$. The radius of the small opening of the i^{th} divided elementary section of the pore is:

$$R_{s,i} = R_0 + (i - 1)l_e \tan\theta, \text{ for } i=1,2,\dots, n \quad (1)$$

The radius of the large opening of the i^{th} divided elementary section of the pore is:

$$R_{l,i} = R_0 + i l_e \tan\theta, \text{ for } i=1,2,\dots, n \quad (2)$$

The average radius of the i^{th} divided elementary section of the pore is:

$$R_{m,i} = R_0 + (i - \frac{1}{2})l_e \tan\theta, \text{ for } i=1,2,\dots, n \quad (3)$$

For a sufficiently large n , the i^{th} divided elementary section of the pore is equivalent to the cylindrical pore with the inner radius $R_{m,i}$ and the axial length l_e . When the passing liquid-pore wall interfacial slippage is neglected, the flow resistance of this equivalent cylindrical pore is (Zhang, 2019):

$$i_{f,i} = \frac{4\eta_{bf}^{eff}(\bar{R}_{m,i})l_e}{\pi\rho_{bf}^{eff}(\bar{R}_{m,i})|S(\bar{R}_{m,i})|R_{m,i}^4} \quad (4)$$

where $\bar{R}_{m,i} = R_{m,i}/R_{cr}$, R_{cr} is the critical inner radius of the cylindrical pore for the liquid to become continuum across the pore radius, ρ_{bf}^{eff} and η_{bf}^{eff} are respectively the average density and the effective viscosity of the confined liquid across the pore radius, and S is the parameter describing the non-continuum effect of the confined liquid across the pore radius ($-1 \leq S < 0$).

In a conical pore of the membrane, all the divided elementary sections as shown in Fig.1(c) are in series connection, the flow resistance of a single conical pore in the membrane is (Zhang, 2019):

$$i_{f,pore} = \sum_{i=1}^n i_{f,i} \quad (5)$$

If the flow resistance of the whole membrane is defined as: $i_{f,men} = \Delta p/q_m$, where Δp is the pressure drop across the membrane and q_m is the mass flow rate through the whole membrane, because of all the conical pores in the membrane in parallel connection, $i_{f,men}$ is equated as (Zhang, 2019):

$$i_{f,men} = \frac{i_{f,pore}}{N_p} \quad (6)$$

where N_p is the number of the conical pores in the whole membrane. It is formulated that $N_p = \lambda_N A_m$, where λ_N is the number density of the conical pore on the membrane surface (in $/m^2$) and A_m is the area of the membrane surface. It can be formulated that $\chi/\lambda_N = \pi R_1^2$, where χ is the pore production rate on the membrane surface. It is then obtained that:

$$\frac{1}{N_p} = \frac{\pi R_1^2}{\chi A_m} \quad (7)$$

Substituting Eq.(7) into Eq.(6) and re-arranging gives that:

$$i_{f,men} = \frac{\pi R_1^2}{\chi A_m} \sum_{i=1}^n i_{f,i} \quad (8)$$

If the dimensionless flow resistance of the membrane is defined as: $I_{f,men} = i_{f,men} \rho \chi A_m R_r^2 / (4\eta l)$ (Zhang, 2019), where R_r is a constant reference radius and ρ and η are respectively the bulk density and the bulk viscosity of the liquid at a given temperature and under low pressures when the liquid is continuum, the dimensionless flow resistance of the membrane is expressed as:

$$I_{f,men} = \sum_{i=1}^n \frac{Cy(\bar{R}_{m,i})(\frac{R_r}{R_0})^2 (\frac{R_1}{R_0})^2}{nCq(\bar{R}_{m,i})|S(\bar{R}_{m,i})|(\frac{R_{m,i}}{R_0})^4} \quad (9)$$

where $Cy(\bar{R}_{m,i}) = \eta_{bf}^{eff}(\bar{R}_{m,i})/\eta$ and $Cq(\bar{R}_{m,i}) = \rho_{bf}^{eff}(\bar{R}_{m,i})/\rho$

4. CALCULATION

First, the proposed model was validated regarding how large values of n should be used. Then, the dimensionless flow resistance of the membrane was calculated for different geometrical shapes of the pore and different liquid-pore wall interactions.

In the calculations, it was taken that $R_r = 10nm$. The formulations of the functions $Cq(\bar{R}_{m,i})$, $Cy(\bar{R}_{m,i})$ and $S(\bar{R}_{m,i})$ are respectively the same with those presented by Zhang (2019) in the earlier study.

For weak, medium and strong passing liquid-pore wall interactions, the values of R_{cr} were respectively taken as 3.5nm, 10nm and 20nm (Zhang, 2019). For the weak, medium and strong liquid-pore wall interactions here studied, the values of the corresponding used parameters have been shown by Zhang (2019).

5. RESULTS AND DISCUSSION

5.1 Validation Of The Model

Figure 2 plots the calculated values of $I_{f,men}$ against n for $\theta = 20^\circ$, $\bar{R}_0 = 0.5$ and different values of λ_1 when the passing liquid-pore wall interaction is weak. Here, $\bar{R}_0 = R_0/R_{cr}$, and $\lambda_1 = R_0/l$. Figure 2 shows that for each λ_1 , when n is sufficiently large, $I_{f,men}$ approaches to a constant value in spite of the variation of n . This indicates that for the present model to simulate the flow in a conical pore, the value of n should be large enough; Otherwise, the calculation will be greatly erroneous. The chosen n value is shown to intimately depend on the value of λ_1 . It was also found that the choosing of the value of n is irrelevant to the liquid-pore wall interaction. In all the present calculations, the value of n is taken as 50000, which is large enough.

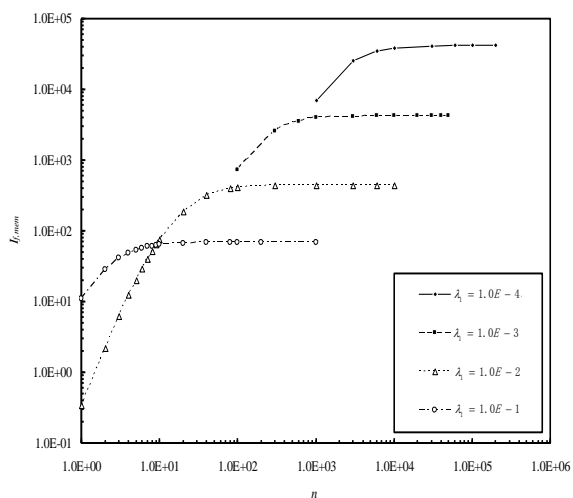
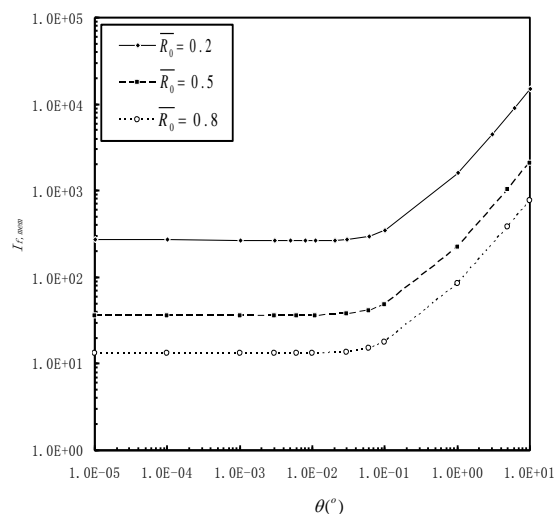


Fig.2 Plots of the value of $I_{f,men}$ against n for $\theta = 20^\circ$, $\bar{R}_0 = 0.5$ and different values of λ_1 when the passing liquid-pore wall interaction is weak.

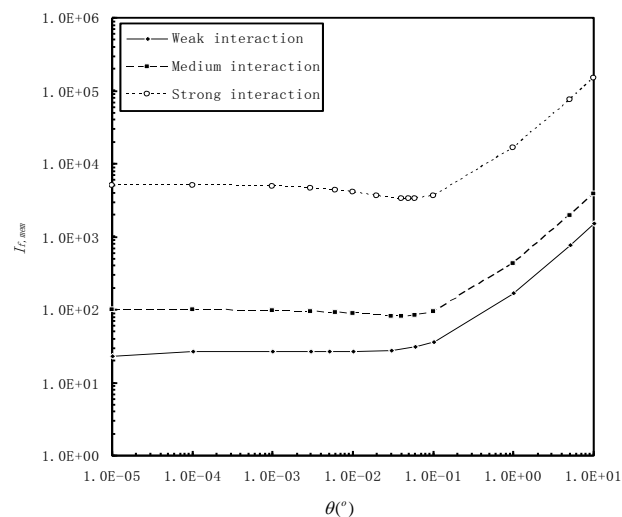
5.2 Dimensionless Flow Resistance Of The Membrane

Figure 3(a) shows the variations of the dimensionless flow resistance ($I_{f,men}$) of the membrane with the cone angle θ of the pore for different \bar{R}_0 values when $\lambda_1 = 1.0E - 3$ and the passing liquid-pore wall interaction is weak. It is shown that there exists the optimum value of θ which yields the lowest flow resistance i.e. the highest flux of the membrane. The value of the cone angle θ deviating from this optimum one increases the flow resistance of the membrane and is thus not beneficial for the performance of the membrane. This optimum θ value was found to be dependent on both the values of \bar{R}_0 and λ_1 and the passing liquid-pore wall interaction.

Figure 3(b) shows the variations of the dimensionless flow resistance ($I_{f,men}$) of the membrane with the cone angle θ of the pore respectively for weak, medium and strong liquid-pore wall interactions when $\lambda_1 = 1.0E - 3$ and $R_0 = 2nm$. For the same operational parameter values, the increase of the interaction strength between the passing liquid and the pore wall significantly increases the flow resistance of the membrane. For a given liquid-pore wall interaction, there exists the optimum value of θ which yields the lowest flow resistance of the membrane. This optimum θ value is practically slightly increased with the increase of the interaction strength between the passing liquid and the pore wall. For the given values of \bar{R}_0 and λ_1 , when the value of θ is optimum, the lowest flow resistance of the membrane is significantly increased with the increase of the interaction strength between the passing liquid and the pore wall.



(a) For the weak passing liquid-pore wall interaction



(b) $R_0 = 2nm$

Fig.3 Plots of the dimensionless flow resistance ($I_{f,men}$) of the membrane against the cone angle θ of the pore when $\lambda_1 = 1.0E - 3$.

5.3 Regression Equations For Calculating The Optimum Value Of The Cone Angle θ Of The Pore

The equations were regressed out for calculating the optimum value of the cone angle θ of the pore as shown above respectively for the weak, medium and strong passing liquid-pore wall interactions. For the weak interaction, the optimum θ value can be calculated from the following equation:

$$\theta_{opt} = \lambda_1(35.6\bar{R}_0^2 - 43.25\bar{R}_0 + 18.23), \quad \text{for } 0.2 \leq \bar{R}_0 \leq 0.9 \quad (10)$$

For the medium interaction, the optimum θ value is calculated from the following equation:

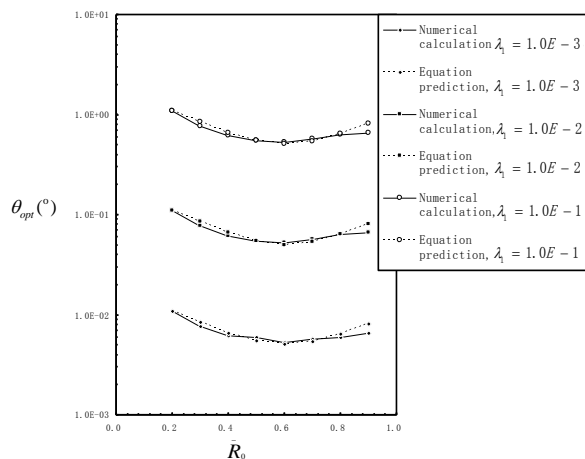
$$\theta_{opt} = \lambda_1(61.1\bar{R}_0^2 - 106.1\bar{R}_0 + 55.76), \quad \text{for } 0.2 \leq \bar{R}_0 \leq 0.9 \quad (11)$$

For the strong interaction, the optimum θ value is calculated from the following equation:

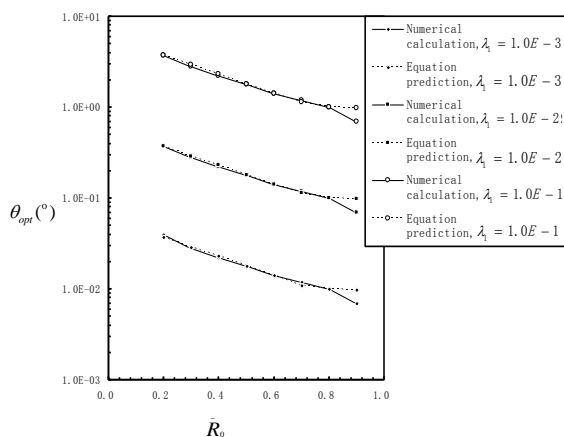
$$\theta_{opt} = -\lambda_1(27.78\bar{R}_0^2 + 33.89\bar{R}_0 - 55.76), \quad \text{for } 0.2 \leq \bar{R}_0 \leq 0.9 \quad (12)$$

The calculated values of θ_{opt} from Eqs.(10)-(12) are in degree.

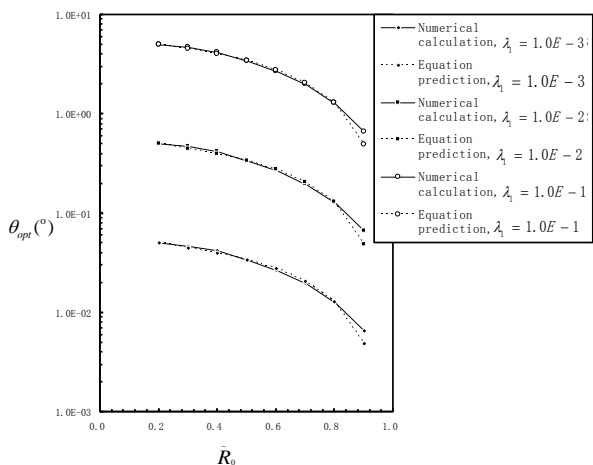
The values of θ_{opt} calculated by Eqs.(10)-(12) are respectively compared with the numerical calculation results in Figs.4(a)-(c). It is shown that the accuracy of the predictions by Eqs.(10)-(12) is satisfactory.



(a) For the weak liquid-pore wall interaction



(b) For the medium liquid-pore wall interaction



(c) For the strong liquid-pore wall interaction

Fig.4 The comparisons of the optimum θ values (θ_{opt}) respectively numerically calculated and equation predicted (by Eqs.(10)-(12)) for the weak, medium and strong liquid-pore wall interactions.

5.4 Regression Equation For Calculating The Dimensionless Lowest Flow Resistance Of The Membrane When The Cone Angle θ Of The Pore Is Optimum

For a given operating condition, when the cone angle θ of the pore is optimum, the flow resistance of the membrane will be the lowest, and the flux of the membrane will thus be the highest. The equations for calculating this dimensionless lowest flow resistance ($I_{f,men,min}$) of the membrane were regressed out as follows:

$$I_{f,men,min} = 2.212\bar{R}_0^2 - 4.462\bar{R}_0 + 3.234, \text{ for the weak liquid-pore wall interaction and } 0.2 \leq \bar{R}_0 \leq 0.9 \quad (13)$$

$$I_{f,men,min} = 3.989\bar{R}_0^2 - 6.819\bar{R}_0 + 3.114, \text{ for the medium liquid-pore wall interaction and } 0.2 \leq \bar{R}_0 \leq 0.9 \quad (14)$$

$$I_{f,men,min} = 6.517\bar{R}_0^2 - 10.539\bar{R}_0 + 3.874, \text{ for the strong liquid-pore wall interaction and } 0.2 \leq \bar{R}_0 \leq 0.9 \quad (15)$$

The values of the dimensionless lowest flow resistance ($I_{f,men,min}$) of the membrane calculated from Eqs.(13)-(15) are respectively compared with the numerical calculation results in Fig.5. It is shown that the calculation accuracy by Eqs.(13)-(15) is satisfactory. The value of $I_{f,men,min}$ is only dependent on the dimensionless radius \bar{R}_0 of the small opening of the conical pore and the passing liquid-pore wall interaction.

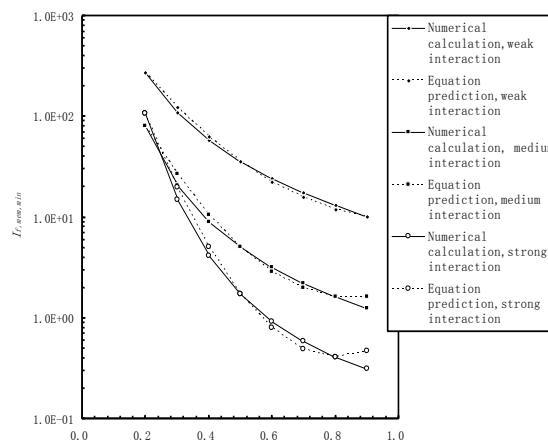


Fig.5 The comparisons of the dimensionless lowest flow resistances $I_{f,men,min}$ of the membrane respectively numerically calculated and equation predicted (by Eqs.(13)-(15)) for the weak, medium and strong liquid-pore wall interactions.

6. CONCLUSIONS

An analysis is developed for the performance of a nanoporous filtration membrane with conical pores which is for a liquid-particle separation, based on the flow equation for a nanoscale flow. The analysis divides a conical nanopore into many elementary sections with a constant very small axial length which can be treated as cylindrical-shaped nanopores with different inner radii. In a conical pore, the divided elementary sections are in series connection; While, in the whole membrane, the conical pores are in parallel connection. Thus, the flow resistance of the whole membrane can be calculated when the flow resistance of an elementary section of the conical pore is calculated. The analysis shows that the flow resistance of the studied membrane is dependent on the radius of the small opening of the conical pore, the cone angle θ of the pore, the membrane thickness and the passing liquid-pore wall interaction. The calculation results show that for a given operating

condition, there is the optimum value of the cone angle θ of the pore which yields the lowest flow resistance i.e. the highest flux of the membrane. The equations for calculating this optimum θ value and for calculating the corresponding dimensionless lowest flow resistance of the membrane were regressed out respectively for weak, medium and strong liquid-pore wall interactions. The obtained results in the present study should be of significant interest to the design and application of nanoporous filtration membranes with conical pores.

7. NOMENCLATURE

A_m	area of the membrane surface
$Cy(\bar{R}_{m,i})$	$\eta_{bf}^{eff}(\bar{R}_{m,i})/\eta$
$Cq(\bar{R}_{m,i})$	$\rho_{bf}^{eff}(\bar{R}_{m,i})/\rho$
$i_{f,i}$	flow resistance of the i^{th} divided section of the cylindrical pore
$i_{f,pore}$	flow resistance of a single conical pore in the membrane
$i_{f,men}$	flow resistance of the whole membrane
$I_{f,men}$	dimensionless flow resistance of the membrane
$I_{f,men,min}$	dimensionless lowest flow resistance of the membrane
l	thickness of the membrane
l_e	axial length of the divided elementary section of the conical pore
n	number of the divided sections of the conical pore
N_p	number of the conical pores in the whole membrane
q_m	mass flow rate through the whole membrane
R_0	radius of the small opening of the conical pore
R_1	radius of the large opening of the conical pore
$R_{s,i}$	radius of the small opening of the i^{th} divided elementary section of the conical pore
$R_{l,i}$	radius of the large opening of the i^{th} divided elementary section of the conical pore
$R_{m,i}$	average radius of the i^{th} divided elementary section of the conical pore
$\bar{R}_{m,i}$	$R_{m,i}/R_{cr}$
\bar{R}_0	R_0/R_{cr}
R_{cr}	critical inner radius of the cylindrical pore for the liquid to become continuum across the pore radius
R_r	constant reference radius
S	parameter describing the non-continuum effect of the confined liquid across the pore radius
θ	cone angle of the conical pore
θ_{opt}	optimum value of the cone angle θ for the lowest flow resistance of the membrane
$\rho_{bf}^{eff}, \eta_{bf}^{eff}$	respectively the average density and the effective viscosity of the confined liquid across the pore radius
Δp	pressure drop across the membrane
λ_N	number density of the conical pore on the membrane surface (in/m^2)
χ	pore production rate on the membrane surface
ρ, η	respectively the bulk density and the bulk viscosity of the liquid at a given temperature and under low pressures when the liquid is continuum
λ_1	R_0/l

REFERENCES

Adiga, S. P., Jin, C., Curtiss, L.A., Monteiro-Riviere, N.A., 2009, "Narayan, R.J. Nanoporous membranes for medical and biological applications." *Nanomed. Nanobiotechnol*, **1**, 568-581.
<https://doi.org/10.1002/wnan.50>

Baker, L.A., Bird, S.P., 2008, "Nanopores: A makeover for membranes." *Nat. Nanotechnol*, **3**, 73-74.
<https://doi.org/10.1038/nnano.2008.13>

Biffinger, J.C., Ray, R., Little, B., Ringeisen, B.R., 2007, "Diversifying biological fuel cell designs by use of nanoporous filters." *Environ. Sci. Tech*, **41**, 1444-1449.
<https://doi.org/10.1021/es061634u>

Cervera, J., Schiedt, B., Ramírez, P., 2005, "A Poisson/Nernst-Planck model for ionic transport through synthetic conical nanopores." *Europhys. Lett*, **71**, 35-41.
<https://doi.org/10.1209/epl/i2005-10054-x>

Desai, T. A., Hansford, D. J., Leoni, L., Essenpreis, M., 2000, "Ferrari, M. Nanoporous anti-fouling silicon membranes for biosensor applications." *Biosens. Bioelec*, **15**, 453-462.
[https://doi.org/10.1016/S0956-5663\(00\)00088-9](https://doi.org/10.1016/S0956-5663(00)00088-9)

Escosura-Muniz, A., Merkoç, A., 2011, "A nanochannel / nanoparticle-based filtering and sensing platform for direct detection of a cancer biomarker in blood." *Small*, **7**, 675-682.
<https://doi.org/10.1002/sml.201002349>

Fissel, W.H., Dubnisheva, A., Eldridge, A.N., Fleischman, A.J., Zydney, A.L., 2009, "Roy, S. High-performance silicon nanopore hemofiltration membranes." *J. Membr. Sci*, **326**, 58-63.
<https://doi.org/10.1016/j.memsci.2008.09.039>

Hinds, B. J., Chopra, N., Rantell, T., Andrews, R., 2004, "Gavalas, V.; Bachas, L. G. Aligned multiwalled carbon nanotube membranes." *Science*, **303**, 62-65.
<https://doi.org/10.1126/science.1092048>

Harrell, C. C., Siwy, Z. S., Martin, C. R., 2006, "Conical nanopore membranes: Controlling the nanopore shape." *Small*, **2**, 194-198.
<https://doi.org/10.1002/sml.200500196>

Jackson, E.A., Hillmyer, M.A., 2010, "Nanoporous membranes derived from block copolymers: From drug delivery to water filtration." *ACS Nano*, **4**, 3548-3553.
<https://doi.org/10.1021/nn1014006>

Mukaibo, H., Horne, L. P., Park, D., 2009, "Controlling the length of conical pores etched in ion - tracked poly(ethylene terephthalate) membranes." *Small*, **5**, 2474-2479.
<https://doi.org/10.1002/sml.200900810>

Scopece, P., Baker, L. A., Ugo, P., Martin, C. R., 2006, "Conical nanopore membranes: solvent shaping of nanopores." *Nanotechnol*, **17**, 3951-3956.
<https://doi.org/10.1088/0957-4484/17/15/057>

Vlassioug, I., Pavel, Y. A., Sergey, N., Dmitriev, K. H., Siwy, Z. S., 2009, "Versatile ultrathin nanoporous silicon nitride membranes." *Proc. Nat. Acad. Sci*, **106**, 21039-21044
<https://doi.org/10.1073/pnas.0911450106>

Zhang, Y. B., 2016, "The flow equation for a nanoscale fluid flow." *Int. J. Heat Mass Transf.*, **92**, 1004-1008.
<https://doi.org/10.1016/j.ijheatmasstransfer.2015.09.008>

Zhang, Y. B., 2018a, "Optimum design for cylindrical-shaped nanoporous filtration membrane." *Int. Commun. Heat Mass Transf*, **96**, 130-138.
<https://doi.org/10.1016/j.icheatmasstransfer.2018.06.003>.

Zhang, Y. B., 2018b, "A tree-type cylindrical-shaped nanoporous filtering membrane." *Front. Heat Mass Transf*, **10**, 16.
<https://dx.doi.org/10.5098/hmt.10.16>

Zhang, Y. B., 2018c, "An optimized tree-type cylindrical-shaped nanoporous filtering membrane." *Front. Heat Mass Transf*, **11**, 25.
<https://dx.doi.org/10.5098/hmt.11.25>

Zhang, Y. B., 2019, "A design method for nanofluidic circuits." *Microsys. Tech.*, **25**, 371-379.
<https://doi.org/10.1007/s00542-018-4029-5>